

# Simulation, Prediction and Compensation of Transient Thermal Deformations of a Reciprocating Linear Slide for F8S Motion Error Separation

**E.H.K. Fung, N.J. Hou, H.F. Yu, W.O. Wong**

The Hong Kong Polytechnic University, Department of Mechanical Engineering  
Hung Hom, Kowloon, Hong Kong, China  
mmhkfung@polyu.edu.hk; hounengjie@gmail.com; 11900610R@connect.polyu.hk;  
mmwowong@polyu.edu.hk

**Abstract** - This study first introduces the prediction of the transient thermal-elastic deformation and the temperature distribution due to friction force derived from the reciprocating motion between the moving parts of a simulation slide model. The FEM results are incorporated into the input motion errors to generate the simulated sensor data for evaluating the Integrated Sensing System (ISS). The procedure for the thermal error compensation is proposed as a pre-processor for the F8S based error separation method. Simulation results show that the F8S based ISS is capable of predicting and compensating the transient thermal errors in a reciprocating linear slide.

**Keywords:** Active error compensation, Linear slide, F8S method, Thermal deformation, Straightness, Roll, Yaw, Profile, On-machine error separation.

## 1. Introduction

Thermal errors (Bryan, 1990; Ramesh et al., 2010) are frequently the biggest problem faced by production engineers as they can account for around 50% of the total positional error of a machine tool. They arise from a combination of internally generated heat such as friction and motor and environmental influences, which unless controlled properly can result in large positional errors (Lee et al., 2003).

In 2010, an efficient method called Fourier-Eight Sensor (F8S) method was proposed by Fung, et al. (2010), to measure the motion errors during machining. The method (Fung et al., 2010; Fung et al., 2014) successfully separates the motion errors into straightness, yawing and rolling errors. Recently, the ISS (Fung et al., 2012; Fung et al., 2013) was designed to reveal the thermal effects and the procedure of thermal error compensation. In this method (Fung et al., 2013), steady state thermal deformation of the table was established using three temperature sensors. However, the transient thermal effect was not fully considered in the simulation study.

The FEM-based transient thermal-structural analysis of a slide model is described in section 2. The FEM simulation procedure is also outlined in this section. Preparation of simulated sensor data is presented in section 3. Error separation using ISS is given in section 4. Simulation results are presented in section 5. Concluding remarks are made in section 6.

## 2. FEM-based Transient Thermal-structural Analysis

In this work, a 3D model of the transient thermal-structural simulation was developed on top of a commercial FEM program called ANSYS® Workbench™ 2.0. It is used to analyze the phenomenon of heat dissipation in the workpieces and its influence on part deformation. The developed system allows users:

- I. To create 3D FEM models of the workpiece configurations;
- II. To apply appropriate machine boundary conditions and loads ;
- III. To perform transient thermal simulation with nonlinear phenomena involving dynamic effects and complex behaviors; and
- IV. To perform transient structural simulation for the reciprocating motion of a linear slide.

The FEM-based analysis using ANSYS takes the following steps.

### Step 1 - Choose Analysis System

In this study, two analysis systems, i.e. Transient Structural Analysis and Transient Thermal Analysis are used.

### Step 2 - Construct Finite-Element Model of Workpieces

The FEM models of the workpieces are created sequentially on the ANSYS DesignModeler. The models consist of a working table and a base with a double guide-ways and a ball screw. The working table and the base are illustrated in Figure 1 and the assembly is shown in Figure 2. For the thermal analysis consideration, structural steel is chosen as the material of the workpieces. The mechanical and thermal properties of steel are listed in Table 1.

Table 1 Mechanical and Thermal Properties of Structural Steel.

Density = 7850 kg/m <sup>3</sup>
Coefficient of Thermal Expansion = 1.2E-05 /°C
Young's Modulus = 2E+11 Pa
Poisson's Ratio = 0.3
Tensile/Compressive Yield Strength = 2.5E+08 Pa
Tensile Ultimate Strength = 4.6E+08 Pa
Specific Heat = 434 J/kg°C
Isotropic Thermal Conductivity = 60.5 W/m°C

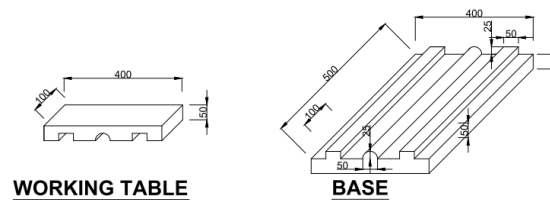


Fig.1. Working Table and Base.

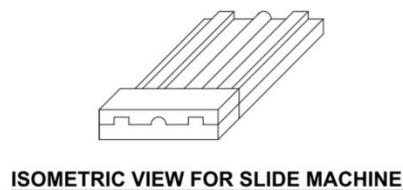


Fig.2. Isometric View for Slide Machine.

### Step 3 - Construct Contact Connection between FEM Models

In this study, the FEM-based simulation analysis aims to figure out how thermal error affects the accuracy of the F8S method. The simulation result of the transient deformation and temperature distribution are focused on the working table which the eight sensors are facing. The other subordinate features of the machine such as the ball screw and the double guide-ways are simplified and incorporated into the base model, which is illustrated in Figure 3 thus reducing the computational time. The connectional contacts between the working table and the base are defined in Figure 3-4. The

salient semi-circular feature of the base representing the ball screw is defined to have frictional contact with the working table with friction coefficient 0.8. The double salient rectangular features of the base representing the double guide-ways are defined to have frictional contacts with the working table with friction coefficient 0.16. Other contact faces between the working table and the base are defined as frictionless connections.

#### **Step 4 - Generate ANSYS Meshing**

To balance the efficiency and accuracy requirements, the adaptive mesh size of 80mm and 15mm are used for the base model and the working table model respectively.

#### **Step 5 - Define Boundary Condition**

In this study, a fixture-workpiece is defined by fastening the bottom surface of the base model to facilitate simulation containing a dynamic motion. The environment temperature is kept at 22°C with a convective heat transfer coefficient of 25W/m<sup>2</sup>K. The initial temperature of all models is defined as 22°C. Heat radiation to the surrounding is ignored.

#### **Step 6 - Create Load and Motion as a Function of Time**

A back-and-forth or reciprocating motion of  $\pm 1$ mm/s along the X-direction is created on the working table. To produce a frictional force, a dummy normal pressure is applied on the working table along Y-direction. The simulation time is 14400s (4 hours) with 144 number of steps (1 step = 100s) which allows the temperature to reach an equilibrium value. At this point, the heat generated by frictional force is equal to that transferred to the surrounding environment.

#### **Step 7 - Perform Transient Thermal-Structural Analysis**

For determining the time-varying deformation and temperature distribution in the workpieces during machining process, the Transient Thermal-Structural Analysis is conducted following the procedure given in (Expertfea, 2013).

#### **Step 8 - Postprocess Numerical Results**

The numerical results are then processed by the Report Generator Module and presented in the form of colored contours and graphs showing the transient temperature distribution and part deformations at specific nodal locations designated by the ISS.

#### **Step 9 - Define Temperature Sensor Placement**

For each thermal mode, it is always desirable to place the temperature sensors according to the following rules:

- (1) Close to the extreme values of the dominant temperature fields or,
- (2) Close to the heat flux sources.

The temperature sensor location is shown in Figure 5.

#### **Step 10 - Define Eight Locations Facing the Displacement Sensors**

The stationary sensor stage is fixed to the table base at specific location. The arrangement of displacement sensors on sensor stage follows the design requirement of the F8S method. All these sensors must face the target profile (Figure 6) of the machine during data collection. The target profile is set to be on one side of the machine. As shown in Figure 8, the sensor location is configured as follows: Total test section length  $L=60$ mm;  $P_1$  is taken to be the zero position or the reference point; distance between  $P_1$  and  $P_2$ ,  $l_2=15.6$ mm; distance between  $P_1$  and  $P_4$  or  $P_6$  and  $P_7$ ,  $l_4=33.8$ mm; distance between the lower sensor row and the rolling axis,  $h_1$  is 4mm; distance between the upper sensor row and the rolling axis,  $h_2$  is 44mm.

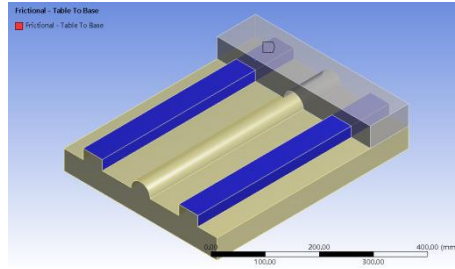


Fig. 3. Contact Surface between working table and base (2 nos. guideway).

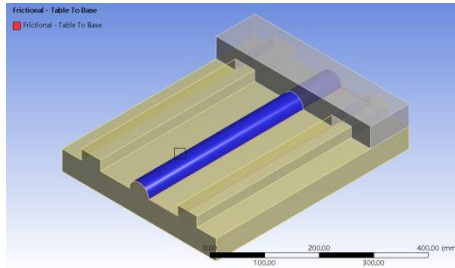


Fig. 4. Contact Surface between working table and base (ball screw).

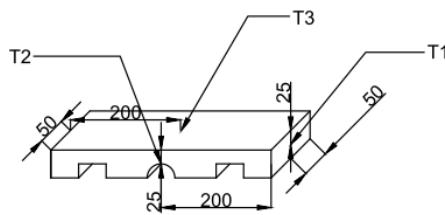


Fig. 5. Temperature Sensor Location.

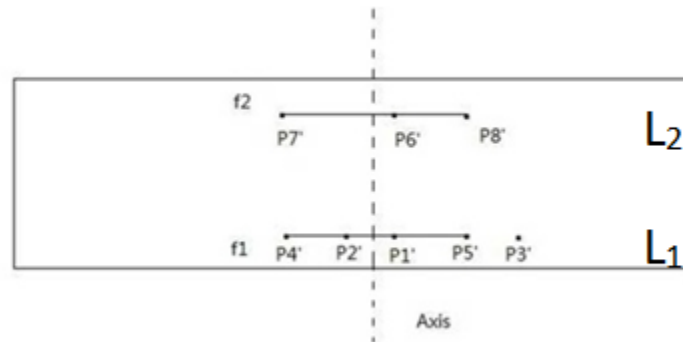


Fig. 6. Profile Facing Sensor Stage.

### 3. Preparation of Simulated Sensor Data

The simulation program (Fung et al., 2010; Fung et al., 2014) combines the predefined  $f_1(\theta), f_2(\theta)$ , the randomly generated  $\tilde{Z}(\theta), \gamma(\theta)$  and  $\omega(\theta)$ , to obtain  $S_1, S_2, \dots, S_8$  as shown in Figure 7. Then, the thermal deformation  $\Delta f_1(\theta), \Delta f_2(\theta)$  are added to  $S_1, S_2, \dots, S_8$  along  $L_1$  and  $L_2$  respectively as indicated in Figure 6, to create the simulated sensor signals  $S_{1T}, S_{2T}, \dots, S_{8T}$ .

#### 3.1. Determination of $\Delta f_1(\theta)$ and $\Delta f_2(\theta)$

The values of thermal deformation at  $t = 100s, 2500s, 4900s, 7300s$  and  $9700s$  for  $P_1', P_2', \dots, P_8'$  are found by ANSYS as described in step 10 of section 2. For the transient study, the thermal deformations along  $L_1$  and  $L_2$  are considered for five motions beginning with  $t = 100s, 2500s, 4900s,$

7300s and 9700s. The sensors will face the same locations at the profile at the start of each motion. The profile changes are assumed to be constant for the 60mm travel. For a particular time, say  $t = 100s$ , the values of thermal deformations along  $L_1$  and  $L_2$  are found by linear interpolations based on the known deformation at the eight points. Interpolation is used to find the approximate profile  $\Delta f_1$  and  $\Delta f_2$  at 301 points, which approximates a complicated function by a simple function.

### 3.2. Formation of $S_{1T}, S_{2T}, \dots, S_{8T}$

The predefined  $f_1(\theta), f_2(\theta), \tilde{Z}(\theta), \gamma(\theta)$  and  $\omega(\theta)$ , which are shown in Figure 7, are combined together with thermal deformation  $\Delta f_1(\theta), \Delta f_2(\theta)$  to create the simulated sensor signals  $S_{1T}, S_{2T}, \dots, S_{8T}$ . The magnitudes of  $\tilde{Z}(\theta), \gamma(\theta)$  and  $\omega(\theta)$  are chosen according to some industrial guidelines.

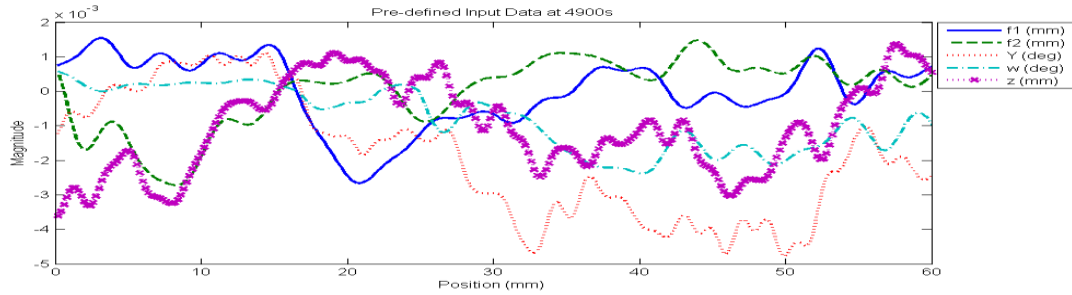


Fig. 7. Predefined inputs (4900s).

The simulated data is now ready for testing the performance of the Integrated Sensing System (ISS).

## 4. Error Separation Using ISS

The estimated values of thermal deformations at  $P_1', P_2', \dots, P_8'$ , are used to generate the approximate  $\Delta f_1', \Delta f_2'$  along  $L_1$  and  $L_2$  respectively for the five starting times  $t = 0s, 100s, 2500s, 4900s, 7300s$  by interpolation. The estimated values are obtained by equation (1) with coefficients found by Linear Square Regression. The calculated  $\Delta f_1', \Delta f_2'$  are subtracted from  $S_{1T}, S_{2T}, \dots, S_{8T}$  to get the new sensor data  $S_{1T}^+, S_{2T}^+, \dots, S_{8T}^+$ . The F8S method is then applied to process  $S_{1T}^+, S_{2T}^+, \dots, S_{8T}^+$  to obtain the profiles of  $f_1^+, f_2^+$  and the motion errors  $Z^+, \gamma^+$  and  $\omega^+$ .

### 4.1. Least Square Regression

The thermal error model of the table is derived to relate the temperature changes collected at the sensor locations ( $\Delta T_1, \Delta T_2$  and  $\Delta T_3$ ) to the estimated thermal deformation of specific points, i.e.  $P_1', P_2', \dots, P_8'$  on that component. The relationship can be represented in the following form:

$$[D] = [\Delta T][A] \quad (1)$$

where  $[D]$  denotes the estimated thermal deformation matrix for  $P_1', P_2'$  to  $P_8'$ ,  $[\Delta T]$  is the measured temperature change matrix, and  $[A]$  is the coefficient matrix found by Least Square Regression using temperatures and deformations obtained at  $t = 100s, 200s, 300s, \dots, 10800s$ .

From equation (1), it can be shown that

$$[A] = \{[\Delta \bar{T}]^T [\Delta \bar{T}]\}^{-1} [\Delta \bar{T}]^T [\bar{D}] \quad \square$$

where  $[\Delta \bar{T}]$  and  $[\bar{D}]$  are the temperature change matrix and the thermal deformation matrix obtained by thermal-structural analysis.

#### 4.2. Estimation of Thermal Deformation at P1', P2', ..., P8'

With the known values of [A] in the above, the estimated deformations at P<sub>1</sub>', P<sub>2</sub>', ..., P<sub>8</sub>', are found using  $[D] = [\Delta T][A]$  where  $[\Delta T]$  is the temperature matrix derived from the readings T<sub>1</sub>, T<sub>2</sub>, T<sub>3</sub>.

#### 4.3. Estimated $\Delta f'_1, \Delta f'_2$ for Thermal Error Compensation

The linear interpolation is applied to determine  $\Delta f'_1, \Delta f'_2$  along L1 and L2 using  $\Delta f'_1$  and  $\Delta f'_2$  at P<sub>1</sub>', P<sub>2</sub>', ..., P<sub>5</sub>' and P<sub>6</sub>', ..., P<sub>8</sub>' respectively. The effects  $\Delta f'_1, \Delta f'_2$  are subtracted from S<sub>1T</sub>, S<sub>2T</sub>, ..., S<sub>8T</sub> to get the new sensor data S<sub>1T</sub><sup>+</sup>, S<sub>2T</sub><sup>+</sup>, ..., S<sub>8T</sub><sup>+</sup> for error separation by F8S.

#### 4.4. Fourier-Eight-Sensor Method (Fung et al., 2010 & 2014)

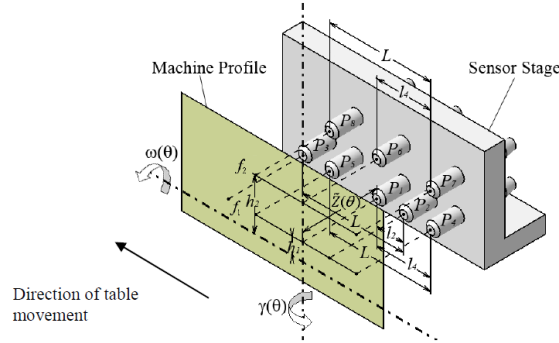


Fig. 8. Sensor Configuration.

Figure. 8 shows the sensor stage used in F8S method which involves eight displacement sensors from P<sub>1</sub> to P<sub>8</sub>. P<sub>1</sub>' to P<sub>8</sub>' are the locations on the working plane which face the sensors P<sub>1</sub> to P<sub>8</sub> respectively (Figure 6). f<sub>1</sub> and f<sub>2</sub> are the profiles of the working plane at ambient temperature facing the lower and upper row sensors respectively. Z is the straightness motion error of the slide;  $\gamma$  and  $\omega$  are the yawing and rolling motion errors of the slide respectively. The F8S method (Fung et al., 2010; Fung et al., 2014) is used to obtain the profiles f<sub>1</sub> and f<sub>2</sub> by using data histories of the eight sensors assuming zero thermal deformation. Other errors can be separated through simple equations based on the calculated profile functions. The procedure for determining f<sub>1</sub>, f<sub>2</sub>, Z,  $\gamma$  and  $\omega$  of a linear slide can be found in (Fung et al., 2010; Fung et al., 2014).

### 5. Simulation Results

#### 5.1. ANSYS Results on Temperature Distribution

The transient temperature distribution of the working table for t=100s, 2500s, 4900s, 7300s and 9700s, are obtained by ANSYS Transient Thermal-Structural Analysis Simulation. The temperature responses of T<sub>1</sub>, T<sub>2</sub>, T<sub>3</sub> are found by this simulation. Typical temperature distribution at t = 4900s and the response of T<sub>1</sub> for 100s < t < 14400s are shown in Figure 9 and 10 respectively.

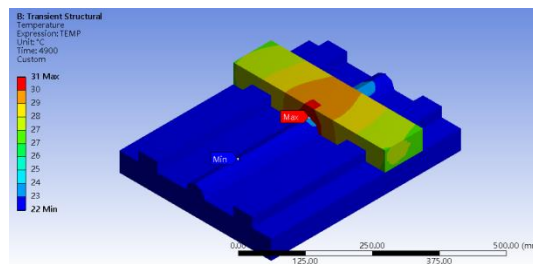


Fig. 9. Temperature Distribution at 4900s.

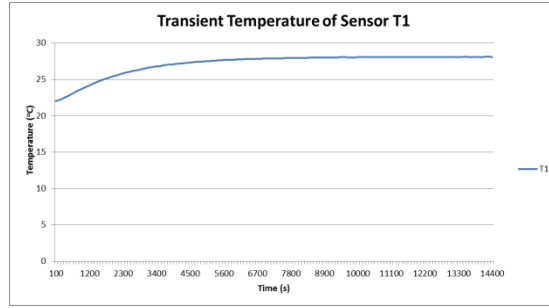


Fig. 10. Temperature Response of T<sub>1</sub>.

### 5.2. ANSYS Results on Thermal Deformations

The detected transient thermal deformations of eight points (P<sub>1</sub>' to P<sub>8</sub>') facing the eight distance sensors P<sub>1</sub> to P<sub>8</sub> of the ISS, i.e.  $\Delta f_1(P_1')$ ,  $\Delta f_1(P_2')$ , ...,  $\Delta f_2(P_7')$ ,  $\Delta f_2(P_8')$ , are obtained by ANSYS Transient Thermal-Structural Analysis simulation. The estimated values i.e.  $\Delta f_1(P_1')$ ,  $\Delta f_1(P_2')$ , ...,  $\Delta f_2(P_7')$ ,  $\Delta f_2(P_8')$ , are calculated based on the measured temperature changes ( $\Delta T_1$ ,  $\Delta T_2$  and  $\Delta T_3$ ) using equation (1). Typical results for  $\Delta f_1(P_1')$  and  $\Delta f_1'(P_1')$  at location P<sub>1</sub>' are shown in Figure 11.

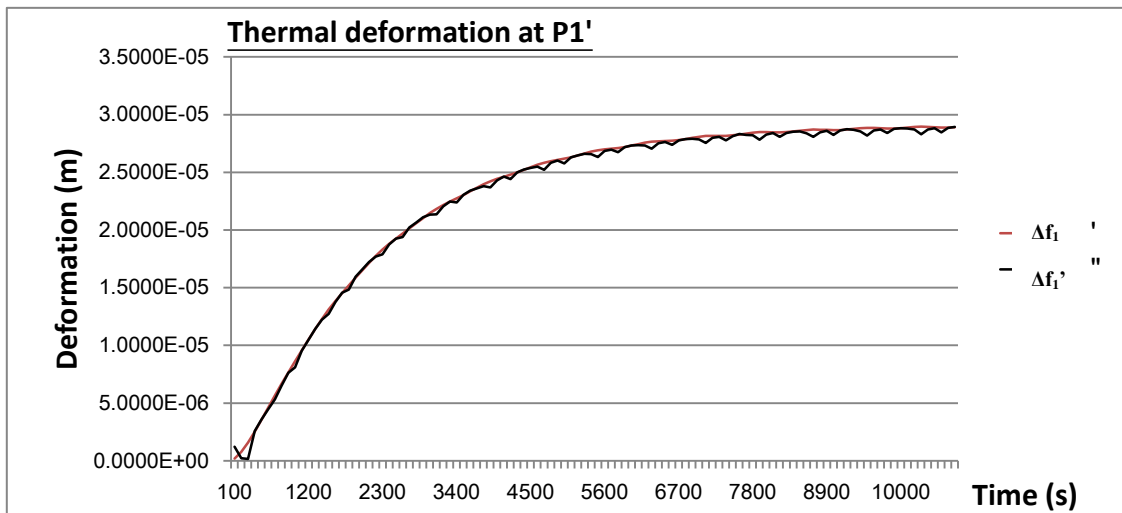


Fig. 11. Comparison between  $\Delta f_1'(P_1')$  and  $\Delta f_1(P_1')$ .

### 5.3. Error Separation based on F8S method

The estimated results with thermal error compensation (Case 2)  $f_1^+$ ,  $f_2^+$ ,  $Z^+$ ,  $\gamma^+$  and  $w^+$  and the results without thermal error compensation (Case 1)  $f_1^*$ ,  $f_2^*$ ,  $Z^*$ ,  $\gamma^*$  and  $w^*$  are obtained by F8S method. At  $t = 4900s$ ,  $Z$ ,  $Z^+$  and  $Z^*$  are compared in Figure 12(a) while  $w$ ,  $w^+$  and  $w^*$  are compared in Figure 12(b). Table 2 lists the result summary.

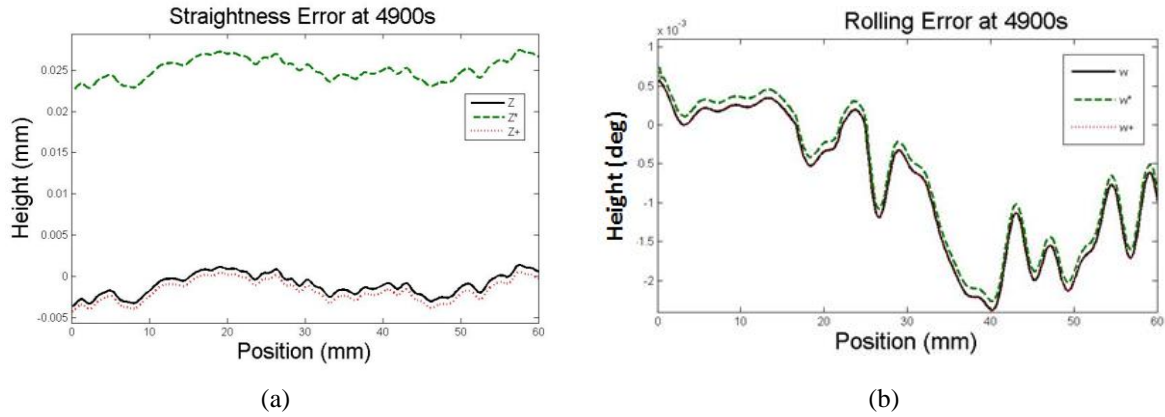


Fig. 12. (a) Straightness Error  $Z$  at 4900s; (b) Rolling Error  $\omega$  at 4900s.

The ANSYS simulation results show that the temperature of the table rose by about  $6^{\circ}\text{C}$  to  $9^{\circ}\text{C}$  and becomes steady at 3 hrs. It is found that the temperature responses at detected locations show similar trends and the increased values are similar to those reported by Rai and Xirouchakis (2009). The maximum thermal deformation is  $2.90 \times 10^{-5}\text{m}$  at P6' and P7' along the travel. It is observed that the ANSYS values and the estimated values at all sensor detected locations show similar trend over the entire reciprocating motion.

At  $t = 4900\text{s}$ , it is found that the calculated results without thermal compensation for the profile and yawing  $f_1^*$ ,  $f_2^*$  and  $\gamma^*$  do not show any significant deviation from their pre-defined values  $f_1$ ,  $f_2$  and  $\gamma$  and the estimated ones with thermal compensation  $f_1^+$ ,  $f_2^+$  and  $\gamma^+$ . However, the average difference for  $Z$  and  $w$  are increased by 36 and 29 times respectively when the thermal effects are not taken into account. On the other hand, the estimated  $Z^+$  and  $\omega^+$  show good agreement with the pre-defined values when the thermal deformations are considered by using the ISS.

Table 2. Maximum and Average Differences for Case 1 and Case 2 ( $t = 4900\text{s}$ ).

Parameters for comparison	Case 1	Case 2
	without thermal effect compensation	With thermal effect compensation
M-dif of f1 (mm)	$4.22 \times 10^{-5}$	$8.01 \times 10^{-6}$
Ave-dif of f1 (mm)	$2.04 \times 10^{-5}$	$3.78 \times 10^{-6}$
M-dif of f2 (mm)	$8.38 \times 10^{-5}$	$5.8 \times 10^{-5}$
Ave-dif of f2 (mm)	$1.24 \times 10^{-5}$	$8.82 \times 10^{-6}$
M-dif of motion (mm)	$2.61 \times 10^{-2}$	$8.26 \times 10^{-4}$
Ave-dif of motion (mm)	$2.61 \times 10^{-2}$	$7.26 \times 10^{-4}$
M-dif of yaw( deg)	$9.29 \times 10^{-5}$	$1.83 \times 10^{-4}$
Ave-dif of yaw( deg)	$9.19 \times 10^{-5}$	$1.82 \times 10^{-4}$
M-dif of roll (deg)	$2.15 \times 10^{-4}$	$1.13 \times 10^{-4}$
Ave-dif of roll (deg)	$1.12 \times 10^{-4}$	$3.86 \times 10^{-6}$

M-dif =  $\max[\text{abs}(\text{predefined data} - \text{calculated data})]$

Ave-dif =  $\text{sum}[\text{abs}(\text{predefined data} - \text{calculated data})]/301$

## 6. Concluding Remarks

An Integrated Sensing System (ISS) is successfully proposed to separate the profiles, the yaw

and the roll errors of a reciprocating linear slide under the effects of transient thermal deformations. The system consists of eight displacement and three temperature sensors. Implementation requires the three major steps:

- (1) Estimation of thermal deformations at eight sensor detected locations based on the three temperature sensor outputs.
- (2) Estimation of the quasi-steady deformation profiles along the scanning direction for a particular travel based on the values at the eight detected locations in (1).
- (3) Subtraction of results in (2) from the sensor outputs followed by error separation using F8S method.

A FEM-based transient thermal-structural simulation using ANSYS is used to generate the transient thermal deformation data for verifying the above implementation. The linear slide model consists of a reciprocating table and a fixed base with rectangular and semi-circular protruding features representing the guide-ways and the ball screw respectively. Simulation results verify that the ISS system performs well under both transient and steady state conditions. The prediction errors for straightness and roll motion have been significantly reduced by about 30 times when the thermal error compensation is incorporated. The efficiency and availability of the machine can be greatly improved as production can be extended to include the three-hour warm-up period.

## Acknowledgements

The authors would like to thank The Hong Kong Polytechnic University for the financial support (Project No. G-YK13) towards this work. Thanks are also due to Mr. CH Cheung, Mr. CM Yu and Mr. WC Mak for their assistance in generating some results presented herein.

## References

- Bryan, J. (1990). International Status of Thermal Error Research. *CIRP Annals – Manufacturing Technology*, 39(2), 645-656.
- Expertfea (2013). Finite Element Analysis Hints and ANSYS Workbench Tutorial – Transient Structural FEA of Heat Generated Between a Piston and a Cylinder. Retrieved from <http://expertfea.com/>
- Fung, E.H.K., Hou, N.J., Zhu, M., Wong, W.O. (2012). A Novel Integrated Sensing System (ISS) for Monitoring Motion Errors of a Precision Linear Slide. “In Proceedings of ASME 2012 International Mechanical Engineering Congress and Exposition,” Texas, Nov 2012, pp. 17-24.
- Fung, E.H.K., Hou, N.J., Zhu, M., Wong, W.O. (2013) .A Novel Method for On-Machine Determination of Slide Motion Errors Considering Thermal Effects. *Applied Mechanics and Materials*, 42, 157-162.
- Fung, E.H.K., Zhu, M., Zhang, X.Z., Wong, W.O. (2010) .An Improved Fourier Eight-Sensor (F8S) Method for Separating Straightness, Yawing and Rolling Errors of a Linear Slide. “In Proceedings of ASME 2010 International Mechanical Engineering Congress and Exposition,” Canada, Nov 2010, pp. 371-378.
- Fung, E.H.K., Zhu, M., Zhang, X.Z., Wong, W.O. (2014) .A Novel Fourier-Eight-Sensor (F8S) Method for Separating Straightness, Yawing and Rolling Motion Errors of a Linear Slide, *Measurement*, 47, 777-788.
- Lee, S.K., Yoo, J.H., Yang, M.S. (2003). Effect of Thermal Deformation on Machine Tool Slide Guide Motion. *Tribology International*, 36(1), 41-47.
- Rai, J.K., Xirouchakis, P. (2009). FEM-based Prediction of Workpieces Transient Temperature Distribution and Deformation during Milling. *International Journal of Advanced Manufacturing Technology*, 42, 429-449.
- Ramesh R., Mannan, M.A., Poo, A.N. (2000). Error Compensation in Machine Tools - a Review, Part II: Thermal Errors, *International Journal of Machine Tools & Manufacturing*, 40, 1257-1284.